J. Phys. B: At. Mol. Opt. Phys. **32** (1999) 4647–4666. Printed in the UK PII: S0953-4075(99)04670-2

Caesium 6P fine-structure mixing and quenching induced by collisions with ground-state caesium atoms and molecules

M Movre, V Horvatic and C Vadla
Institute of Physics, Bijenicka 46, 10000 Zagreb, Croatia

Received 1 June 1999, in final form 27 July 1999

Abstract. Applying the cw laser fluorescence method, the cross sections for the fine structure mixing and quenching of the Cs 6P state, induced by collisions with ground-state caesium atoms and molecules, have been measured. Caesium atoms were optically excited to the $5D_J$ states via quadrupole-allowed $6S_{1/2} \rightarrow 5D_J$ transitions, while the resonance states were populated by the radiative and collisional $5D_J \rightarrow 6P_J$ transitions. The relative populations of the Cs $6P_J$ sublevels, as well as ratio of the $5D_{3/2}$ to $6P_{3/2}$ populations, were measured as a function of the caesium ground-state number density. From these measurements we obtained the cross section of $(14 \pm 5) \times 10^{-16}$ cm^2 at $T = 585$ K for the process $Cs(6P_{1/2}) \rightarrow Cs(6P_{3/2})$ induced by collisions with ground-state caesium atoms. The applied experimental approach enabled the determination of the effective spontaneous rates for the $6P_J$ states which are in agreement with the predictions of Holstein's theory. The cross sections for quenching of $6P_J$ by caesium atoms and molecules were measured at $T = 635$ K and the obtained values are $(1.6 \pm 1.4) \times 10^{-16}$ cm^2 and $(1210 \pm 260) \times 10^{-16}$ cm^2, respectively. Using recently calculated Cs* + Cs potentials we performed an analysis which shows a good agreement between the measured values and the theoretical estimates.

1. Introduction

Investigations on excitation energy transfer (EET) processes give important contributions to our understanding of the dynamics of inelastic collisions in gases and represent a very sensitive test for our knowledge of potentials between atoms or molecules involved in collision processes. In general, studies of EET collisions concern the determination of the cross sections for the collisional processes between two particles A and B, being in different excited states before and after collision. These processes can be schematically described as

$$A(m) + B(n) \rightarrow A(m') + B(n'). \tag{1}$$

Usually, the number of such processes per unit volume and time are defined in the product form $N_A(m)N_B(n)v_{A-B}\sigma$, where $N_A(m)$ and $N_B(n)$ are the number densities of the particles in initial states m and n, respectively, v_{A-B} is the relative velocity of the collisional partners and σ is the velocity-dependent cross section for a particular reaction.

The alkali metals are known to be the most convenient subjects for studying these effects both from the experimental and the theoretical point of view. The EET in collisions between an excited alkali atom and a similar or dissimilar ground-state alkali atom has been the subject of numerous experimental and theoretical investigations in the last four decades. A complete review of experimental and theoretical studies in this field up to 1975 (Krause 1975) shows that even in the case of the simplest systems, such as alkali atoms, these investigations are characterized by significant disagreements between the results of different groups of

0953-4075/99/194647+20$30.00

investigators and, in addition, there is pronounced disagreement between experimental and theoretical results. Laser spectroscopy methods, introduced in the last two and a half decades, have enabled more sensitive measurements. However, radiation trapping effects, uncertainties in determination of particle number densities as well as an incomplete insight into all the attendant collisional mechanisms of a particular system, remained as main sources of systematic errors in such experiments.

In the last decade, the investigations of collisional energy transfer between alkali atoms have shifted to energy-pooling (EP) processes, i.e. collisions involving two excited atoms producing one atom in the ground state and the other in a highly excited state. Very recently, quantitative experimental results for the cross sections for EP collisions involving two excited caesium atoms were published (Jabbour *et al* 1996, Vadla *et al* 1996, Vadla 1998). In order to define the optimum experimental conditions in such EP experiments, a knowledge about cross sections for simpler transfer processes in the investigated system is often required. For instance, collisional mixing processes between initial states for a certain EP process determine whether the measurements under particular experimental conditions would yield J-selective or J-nonselective EP cross sections. However, even for the simplest EET processes in caesium, i.e. collisions between atoms excited to the $6P_J$ states and ground-state atoms, inconsistencies in the published data still persist (Bunke and Seiwert 1962, Czajkowski and Krause 1965). A few years ago Sasso *et al* (1992) published the first results for quenching of the 6P states caused by collisions with caesium ground-state atoms and molecules. During the preparation of this manuscript, we have learned (Huennekens and Sasso 1998) that the quenching cross sections reported by Sasso *et al* (1992) were in error (see section 5.2). As for the fine-structure mixing of the Cs $6P_J$ states, to our knowledge the cross section data can be found only in two pioneering works (Bunke and Seiwert 1962, Czajkowski and Krause 1965). These two results put together suggest that the cross sections for the $6P_{1/2} \rightarrow 6P_{3/2}$ and $6P_{3/2} \rightarrow 6P_{1/2}$ processes both decrease (the former mildly, and the latter by more than a factor of two) as the temperature increases in the range between 323 and 473 K. This is not in accordance with the expected temperature dependence (increase for endothermic and mild decrease for exothermic processes).

For the above-mentioned reasons, in the course of EP experiments (Vadla 1998), we performed measurements of EET processes involving caesium atoms excited to the $6P_J$ state and colliding with caesium ground-state atoms or molecules. The cross section for the fine-structure mixing of the Cs resonance $6P_J$ states due to ground-state caesium atoms

$$\mathrm{Cs}(6\mathrm{P}_{1/2}) + \mathrm{Cs}(6\mathrm{S}) \rightarrow \mathrm{Cs}(6\mathrm{P}_{3/2}) + \mathrm{Cs}(6\mathrm{S}), \tag{2}$$

and the cross sections for quenching due to caesium molecules

$$\mathrm{Cs}(6\mathrm{P}) + \mathrm{Cs}_2 \rightarrow \mathrm{Cs}(6\mathrm{S}) + \mathrm{Cs}_2^*, \tag{3}$$

as well as due to caesium ground-state atoms

$$\mathrm{Cs}(6\mathrm{P}) + \mathrm{Cs}(6\mathrm{S}) \rightarrow \mathrm{Cs}(6\mathrm{S}) + \mathrm{Cs}(6\mathrm{S}), \tag{4}$$

were measured. The method we employed differs from methods used previously by other authors. It enables simultaneous determination of the cross sections for various processes (mixing, quenching, EP) and it is not demanding regarding the experimental conditions under which it is to be used. Also, it circumvents the necessity of applying any theory of resonant radiation trapping in advance. Additionally, we performed a semi-quantitative theoretical study of the measured processes.

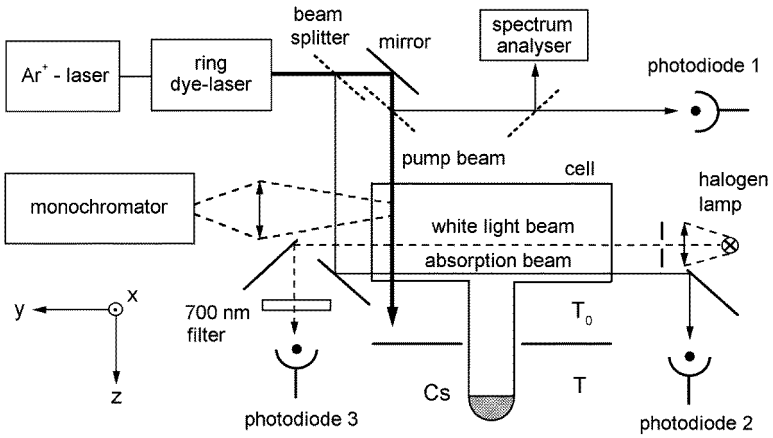

Figure 1. Experimental arrangement.

2. Experiment and methods

2.1. Experimental arrangement

A schematic diagram of the experimental set-up used is shown in figure 1. Pure caesium metal was contained in the finger of the evacuated cylindrical Pyrex glass cell. The inner diameter and the inner length of the cell were $d = 2.7$ cm and $L = 13$ cm, respectively. The cell was placed in a two-chamber resistively heated oven. The temperatures of the cell and the cell finger were measured by iron–constantan thermocouples. The temperature T_0 of the cell was kept constant (585 K and 635 K for 6P fine-structure mixing and quenching measurements, respectively) its value being about 30 K higher than the highest temperature of the caesium metal bath in the cell finger. By changing the temperature T of the metal bath, the caesium number density in the cell was varied in the range between 3×10^{14} and 5×10^{16} cm^{-3}. In order to control the change in transparency of the cell windows, the absorption of the white light beam at 700 nm was measured.

Caesium ground-state atoms were excited to the $5D_J$ states via dipole-forbidden, but quadrupole-allowed $6S_{1/2} \rightarrow 5D_J$ transitions using a cw single-mode (linewidth about 1 MHz), frequency-stabilized ring-dye laser (Spectra Physics, model 380, dye: DCM) pumped by 5 W all-lines argon ion laser (Spectra Physics, model 2020). The frequency of the ring laser was tuned to the centre of the stronger hyperfine component of either the 685 nm line ($6S_{1/2} \rightarrow 5D_{5/2}$ transition) or 689 nm line ($6S_{1/2} \rightarrow 5D_{3/2}$ transition). The resonant $6P_J$ states were populated due to the radiative and collisional depopulation of the $5D_J$ states. The laser beam was split in three parts. The main part, henceforth called the pump beam, was shone through the cell perpendicular to its axis at a distance of 5 mm from the cell window. The pump beam had a diameter of about 1 mm and maximum power of 50 mW at 685 nm. The second part (power: a few μW) of the split laser beam was used to measure the absorption at the pump transitions, needed for the caesium ground-state density determination. Using the triple, double and single pass of the absorption beam along the cell axis, as well as the pass perpendicular to the cell axis, the absorption lengths used (from 2.7 to 39 cm) enabled us to determine the caesium ground-state number densities spanning over two orders of magnitude. The third part of the split laser beam was used to control the laser frequency and power stability.

The cylindrical fluorescence zone (length: 5 mm) was imaged in 1:2 ratio onto the entrance

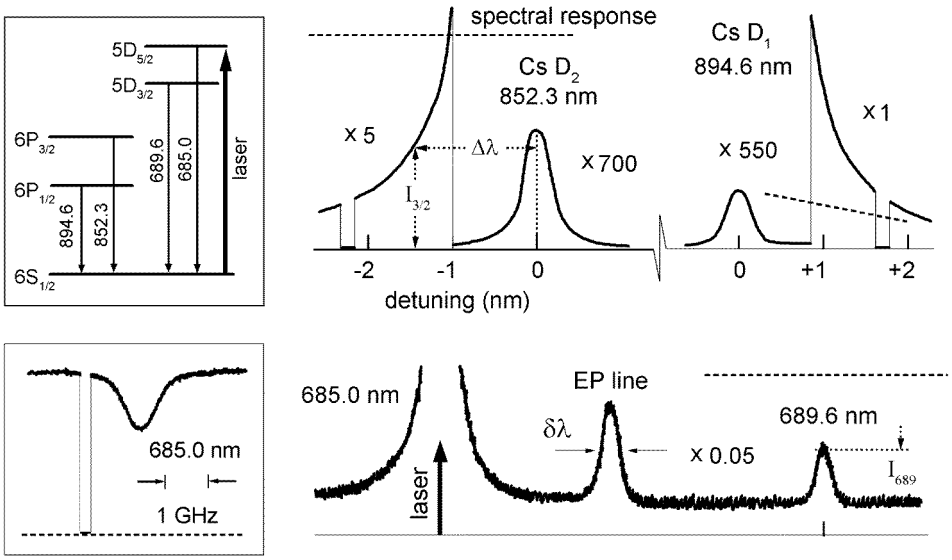

Figure 2. Typical measured spectra of Cs: upper part, fluorescence of the resonance D1 and D2 lines; lower part, fluorescence of the pumped 685 nm and sensitized 689.6 nm components of the Cs 5D doublet. The EP line at 687.2 nm ($7F_J \rightarrow 5D_{5/2}$ transition) is also indicated. The spectra were obtained by scanning the monochromator while the pump laser frequency was locked to the centre of the 685.0 nm line. The upper inset shows the partial caesium term diagram with the relevant transitions indicated. The absorption on the pump transition is shown in the lower inset.

slit of a 1 m McPherson monochromator and the fluorescence signals were detected by a RCA photomultiplier (type C31034A). The spectral response of the detection system was determined using a calibrated tungsten-ribbon lamp (type W2KGV22i). With slit widths of 0.25 mm, the band pass of the monochromator was 0.21 nm at wavelength 700 nm. The monochromator slits were parallel to the fluorescence zone axis (the z-direction, see figure 1) and with the aforementioned slit width only the central slab (thickness: 0.5 mm) of the fluorescence zone was observed. Typical obtained spectra are shown in figure 2. To determine the axially symmetric spatial distributions of the atoms excited to the 5D and 6P states, the fluorescence intensities of the sensitized quadrupole line and the intensities of the optically thin resonance line wings were measured, respectively. For this part of the measurement the entrance slit was narrowed to 0.1 mm and the observed layer within the fluorescence zone was discriminated by moving the imaging lens in the x-direction (see figure 1).

2.2. Determination of the caesium ground-state number density

The caesium ground-state number densities were determined by the measurements of the peak optical depths $\kappa_{SD}(\nu_{SD})L$ at the central frequency ν_{SD} of the 6S $\rightarrow$ 5D pump transition. The profiles of the caesium quadrupole lines measured in this work are generally of the Voigt type, i.e. a convolution of a Gaussian (Doppler broadening) and a Lorentzian (pressure and natural broadening) function. The peak absorption coefficient is of the form $\kappa_{SD}(\nu_{SD}) = \kappa_0 H(0, a)$ (Mitchell and Zemansky 1971), where κ_0 is the Doppler peak absorption coefficient, and $H(\Delta\nu, a)$ is the Voigt function with parameter $a = \Gamma_\nu/2\Delta\nu_D$ (Γ_ν is the Lorentzian FWHM expressed in Hertz, and $\Delta\nu_D = (\nu_{SD}/c)\sqrt{2kT/M}$ is the Doppler constant). At the highest caesium number densities in the present work ($\sim 5 \times 10^{16}$ cm^{-3}) we obtained the value $a \approx 0.1$

from the measured line profiles of the hyperfine components of the Cs quadrupole lines. In this case, the Voigt function in the line core is practically equal to the Gaussian function and its value $H(0, 0.1) \approx 1$. Therefore, the quadrupole line profiles in the whole range of applied caesium number densities can be fairly regarded as pure Doppler profiles. Thus, the number density of the ground-state caesium atoms N_0 can be determined from the measured peak absorption coefficient at the wavelength of the pump 6S $\rightarrow$ 5D transition using the following relation:

$$N_0 = \kappa_{SD}(\nu_{SD}) \frac{m_e \nu_{SD}}{e^2 f_{SD}} \sqrt{\frac{2kT}{\pi M}}, \tag{5}$$

where N_0 is the caesium ground-state number density, f_{SD} is the line oscillator strength, ν_{SD} is the frequency of the line centre.

For the evaluation of caesium number densities we used the quadrupole oscillator strengths measured by Niemax (1977), who reported the total oscillator strengths of Cs quadrupole lines $f_{685} = (5.65 \pm 0.28) \times 10^{-7}$ and $f_{689} = (3.28 \pm 0.25) \times 10^{-7}$. The oscillator strengths of the stronger hyperfine components amount to $\frac{9}{16}$ of the total values. For example, at the typical temperature $T = 600$ K, the caesium ground-state number density N_0 can be determined by using the formula $N_0\ (\mathrm{cm}^{-3}) = 8.46 \times 10^{16} \times \kappa^s_{685}(\nu_{SD})$, where the peak absorption coefficient $\kappa^s_{685}(\nu_{SD})$ of the stronger hyperfine component of the 685 nm line is expressed in units of cm^{-1}. It should be mentioned that only a small fraction (less than 1%) of the ground-state atoms was transferred to the excited states by laser pumping and the measured ground-state number density is practically equal to the total caesium number density.

The measurement of the caesium ground-state number density via the absorption coefficient of the pump line is very convenient because it enables simultaneous measurements of the fluorescence line intensities. In order to check the accuracy of the applied method, which depends on the accuracy of the used oscillator strength, we determined separately the caesium ground-state number density by the white light absorption measurements of the absorption coefficient in the blue quasi-static wing of the self-broadened Cs D2 line. An excellent agreement (within 5%) between these two approaches has been found. The method for determination of caesium vapour density via absorption in the resonance line quasi-static wings was tested by Horvatic *et al* (1993) and the accuracy of the obtained data for caesium atom number density was found to be $\pm 3\%$.

2.3. Determination of relative number densities in excited caesium states

Typical EET experiments involve atoms excited in the first resonance states and in most cases measurable transfer signals can be obtained at atomic number densities for which the resonance radiation is optically thick and trapped. This fact requires the absorption corrections and the determination of the effective radiative rates either by calculations applying the radiation trapping theories to particular experimental conditions or by additional time-resolved effective lifetime measurements. The method we used for determination of population density ratios involving the Cs resonance state populations circumvents this problem.

The relative number densities of the excited caesium atoms were determined by use of the resonance line wings as a quasi-continuous relative standard of radiation. As reported by Vadla *et al* (1996), this approach is especially convenient for measurements performed at relatively high ground-state number densities, where the resonance lines are optically thick and strongly trapped in the line core and exhibit very pronounced quasi-static broadening in the line wings.

According to Mitchell and Zemansky (1971) the absorption coefficient is related to the number density $\mathrm{d}N_\mathrm{a}$ of the absorbing species (in our case quasi-molecules), capable of

absorbing in the frequency range $(\nu, \nu + \mathrm{d}\nu)$, through the relation

$$\kappa(\nu)\,\mathrm{d}\nu = \frac{\lambda^2}{8\pi} A \frac{g_\mathrm{e}}{g_\mathrm{a}}\,\mathrm{d}N_\mathrm{a}, \tag{6}$$

where g_a and g_e are the statistical weights of the lower (absorbing) and upper (emitting) state of the quasi-molecule, respectively, and A is the Einstein spontaneous emission coefficient. Similarly, the power emitted per unit volume in the frequency range $(\nu, \nu + \mathrm{d}\nu)$ is given by

$$P(\nu)\,\mathrm{d}\nu = h\nu A\,\mathrm{d}N_\mathrm{e}, \tag{7}$$

where $\mathrm{d}N_\mathrm{e}$ labels the number density of emitting quasi-molecules. By combining equations (6) and (7) we obtain

$$P(\nu) = h\nu \frac{8\pi}{\lambda^2} \frac{g_\mathrm{a}}{g_\mathrm{e}} \frac{\mathrm{d}N_\mathrm{e}}{\mathrm{d}N_\mathrm{a}} \kappa(\nu). \tag{8}$$

In the quasi-static approximation the number densities of homonuclear pairs are described by

$$\mathrm{d}N_\mathrm{a} = \tfrac{1}{2} N_0^2 4\pi R^2\,\mathrm{d}R \exp(-V_0(R)/kT), \tag{9}$$

$$\mathrm{d}N_\mathrm{e} = N_J N_0 4\pi R^2\,\mathrm{d}R \exp(-V_J(R)/kT), \tag{10}$$

where V_0 and V_J are the corresponding interatomic potentials, N_0 and N_J are the atom number densities of the ground and first resonance state, respectively. The molecular statistical weights are $g_\mathrm{a} = g_0 \times g_0$ and $g_\mathrm{e} = 2g_J \times g_0$. Here, g_0 and g_J label the atomic statistical weights of the ground and first resonance state, respectively. Finally, with the preceding expressions and definitions incorporated, equation (8) acquires the form

$$P(\nu) = h\nu \frac{8\pi}{\lambda^2} \frac{g_0}{g_J} \frac{N_J}{N_0} \kappa(\nu) \exp(-h\Delta\nu/kT), \tag{11}$$

where $h\Delta\nu = V_J(R) - V_0(R)$.

The absorption coefficient in the outer quasi-static wings of the first resonance alkali lines is of the form (Horvatic *et al* 1993)

$$\kappa(\nu) = \frac{4\pi^2 e^2}{3m_e c} f_J C_3^J \frac{N_0^2}{(\Delta\nu)^2}. \tag{12}$$

Here, f_J is the line oscillator strength, and C_3^J (expressed in $\mathrm{cm}^3\ \mathrm{s}^{-1}$) is the effective resonance interaction constant.

If we assume that the radiation emitted in the optically thin quasi-static wings is registered at frequency detuning $\Delta\nu$ which is large in comparison with the monochromator band pass $\delta\nu$, then the wing intensity can be regarded constant within the interval $(\nu, \nu + \delta\nu)$ and the measured intensity I_J emitted from the volume ΔV can be, according to equations (11) and (12), expressed in the form

$$I_J(\pm|\Delta\nu|) \propto \varepsilon_J h\nu_J \beta_J N_J N_0 \exp[\mp h|\Delta\nu|/kT] \frac{\delta\nu}{(\Delta\nu)^2} \Delta V. \tag{13}$$

Here, the sign (+) stands for $J = \frac{3}{2}$ (blue wing) and (−) for $J = \frac{1}{2}$ (red wing), ε_J labels the efficiency of the detection system at the transition frequency, and $\beta_J = 64\pi^3 e^2 f_J C_3^J/(3m_e c\lambda_J^2(2J+1))$. Theoretical results (Movre and Pichler 1980) for caesium resonance interaction constants C_3^J for the $6\mathrm{S}_{1/2} \rightarrow 6\mathrm{P}_J$ transitions have had thorough experimental confirmation (Horvatic *et al* 1993). According to these works the effective $C_3^{1/2}$ and $C_3^{3/2}$ constants for caesium D lines are 3.4×10^{-9} and $5.0 \times 10^{-9}\ \mathrm{cm}^3\ \mathrm{s}^{-1}$, respectively. These values and the line shape described by equation (12) are, according to Movre and Pichler

(1980), valid for outer wings of the resonance doublet and for the detuning from the line centre $\Delta\nu$ smaller than one-third of the fine-structure splitting. Using these data for the caesium C_3^J constants, we find the values $\beta_{1/2} = 0.40$ cm^3 s^{-2} and $\beta_{3/2} = 0.67$ cm^3 s^{-2}.

According to equation (13), the population ratio for the fine-structure levels of the resonance state reads:

$$\frac{N_{1/2}}{N_{3/2}} = \frac{\varepsilon_{3/2}}{\varepsilon_{1/2}} \cdot \frac{I_{1/2}(-|\Delta\nu|)}{I_{3/2}(+|\Delta\nu|)} \frac{\nu_{3/2}}{\nu_{1/2}} \frac{\beta_{3/2}}{\beta_{1/2}} \exp[-2h|\Delta\nu|/kT]. \tag{14}$$

The measurement of optically thin resonance line wings intensities yields the relative population density in resonance $n\mathrm{P}_J$ states. On the other hand, by comparing the line intensity $I_{mn} \propto \varepsilon_{mn} h\nu_{mn} A_{mn} N_m \Delta V$ of an optically thin line of the $m \to n$ transition, with the resonance wing intensity, we obtain the formula for the determination of the upper-state-to-resonance-state population ratio:

$$\frac{N_m}{N_J} = \frac{\varepsilon_J}{\varepsilon_{mn}} \frac{I_{mn}}{I_J(\pm|\Delta\nu|)} \frac{\nu_J}{\nu_{mn}} \frac{\delta\nu}{(\Delta\nu)^2} \frac{\beta_J}{A_{mn}} N_0 \exp[\mp h|\Delta\nu|/kT]. \tag{15}$$

The above considerations were made assuming the isotropic number densities of excited states. In the case of inhomogeneous number densities, the integral $\int N_m(\vec{r})\,\mathrm{d}V$ over the observation volume should replace the product $N_m \Delta V$. For our experimental conditions the population densities were constant along the pump beam axis and axially symmetric. Using the distribution function $f_m(r)$ normalized to unity at the beam axis ($r = 0$), the position dependent population density can be described with $N_m(\vec{r}) = N_m \int f(r)\,\mathrm{d}V$, where N_m denotes the population density at the beam axis. Taking these volume effects into account, the modified equations (14) and (15) are related to the population ratios at the beam axis. As we shall show, the spatial distributions of the $6\mathrm{P}_J$ states are identical. Thus, equation (14) remains formally the same, while equation (15) becomes

$$\frac{N_m}{N_J} = \frac{\varepsilon_J}{\varepsilon_{mn}} \frac{I_{mn}}{I_J(\pm\Delta\nu)} \frac{\nu_J}{\nu_{mn}} \frac{\delta\nu}{(\Delta\nu)^2} \frac{\beta_J}{A_{mn}} N_0 \exp[\mp h|\Delta\nu|/kT] \frac{\int f_J(r)\,\mathrm{d}V}{\int f_m(r)\,\mathrm{d}V}. \tag{16}$$

It should be noted that this method is based on the accurate data for the alkali resonance line self-broadening parameters, and is applicable to other systems with known parameters of quasi-static line broadening. The C_3^J constants given above essentially depend on the value of the oscillator strength $f_{3/2}$ for the $6\mathrm{S}_{1/2} \to 6\mathrm{P}_{3/2}$ transition (see Movre and Pichler 1977, Movre and Pichler 1980, Horvatic *et al* 1993). In obtaining C_3^J values the oscillator strength reported by Link (1966) was used, which agrees within 0.5% with the values that can be deduced from the recent precision $6\mathrm{P}_{3/2}$ lifetime measurements (Tanner *et al* 1992, Rafac *et al* 1994, Young *et al* 1994). The latest theoretical calculations (Marinescu and Dalgarno 1995) would yield $f_{3/2}$ and C_3^J constants that are 4.5% higher than those used here. The choice of the C_3^J values is of no importance for the population ratio defined by relation (14). The use of the results of other authors would affect the ratio given by expression (15) by 1% (Tanner *et al* 1992, Rafac *et al* 1994, Young *et al* 1994) or 9% (Marinescu and Dalgarno 1995).

3. Mixing of the Cs $6\mathrm{P}_J$ states

3.1. Rate equations and the method

Figure 3 shows the partial term scheme of caesium which includes the rates relevant for population and depopulation of the resonant $6\mathrm{P}_J$ states. The states $6\mathrm{S}_{1/2}$, $6\mathrm{P}_{1/2}$, $6\mathrm{P}_{3/2}$, $5\mathrm{D}_{3/2}$, and $5\mathrm{D}_{5/2}$ are denoted as states 0–4, respectively. The radiative and collisional fine-structure mixing rates (due to ground-state caesium atoms) for $m \to n$ transitions are denoted by A_{mn} and R_{mn}, respectively, while the quenching rates for particular m states are labelled Q_m.

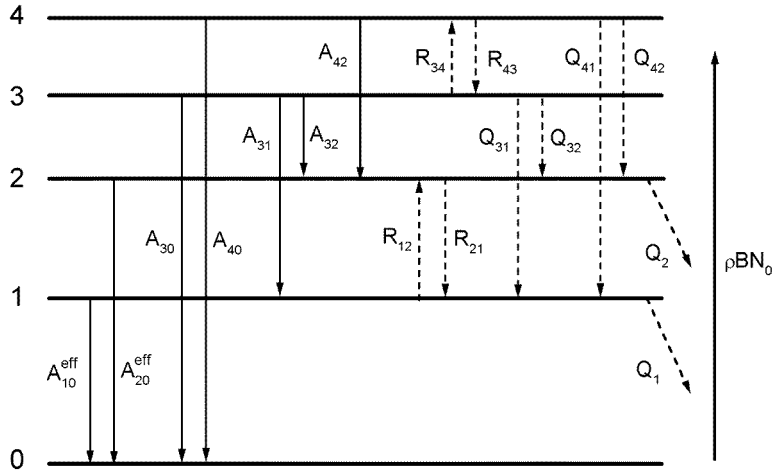

Figure 3. Partial term scheme of caesium, including the radiative (A), collisional (R), and quenching (Q) rates relevant for the population and depopulation of the Cs $5D_J$ and $6P_J$ states. The states $6S_{1/2}$, $6P_{1/2}$, $6P_{3/2}$, $5D_{3/2}$ and $5D_{5/2}$ are denoted as states 0–4, respectively.

In our experimental conditions, the radiative 5D $\rightarrow$ 6P transition was not trapped and the corresponding A_{mn} rates are equal to the natural radiative rates. Using the data for the quadrupole and dipole oscillator strengths published by Niemax (1977) and Hansen (1984), respectively, we calculated the following values for the radiative rates A_{mn}: $A_{30} = 23.0\ \mathrm{s}^{-1}$, $A_{40} = 26.8\,\mathrm{s}^{-1}$, $A_{31} = 9.0\times10^5\,\mathrm{s}^{-1}$, $A_{32} = 1.0\times10^5\,\mathrm{s}^{-1}$, and $A_{42} = 7.2\times10^5\,\mathrm{s}^{-1}$. In contrast to 5D $\rightarrow$ 6P, the resonance $6P_J \rightarrow 6S_{1/2}$ radiation was optically thick and strongly trapped. Therefore, the radiative relaxation of the $6P_J$ states is represented by effective radiative rates A_{10}^{eff} and A_{20}^{eff}.

The fine-structure mixing rates R_{nm} due to collisions with the Cs ground-state atoms are of the form $N_0 v_{\mathrm{Cs-Cs}} \sigma_{mn}$. The quenching of the $5D_J$ states is ascribed to 5D $\rightarrow$ 6P depopulation due to collisions with the ground-state atoms, since the quenching to the ground state is less probable because of the large energy difference between the initial and final states. Thus, each of the Q_m ($m = 3, 4$) rates branches to the Q_{m1} and Q_{m2} portions. We assume the resonance states to be collisionally depopulated by the rates Q_1 and Q_2 which include the $6P_J \rightarrow 5D_J$ back transfer and the quenching due to collisions with the ground-state caesium atoms and molecules.

Within the frame of the present experiment we have also measured (Vadla *et al* 1999) the cross sections σ_{43} and σ_{D} for the fine-structure mixing and quenching of the Cs 5D state. The values obtained are: $\sigma_{43} = (45 \pm 15) \times 10^{-16}\ \mathrm{cm}^2$ and $\sigma_{\mathrm{D}} = (30 \pm 10) \times 10^{-16}\ \mathrm{cm}^2$ at $T = 585$ K. The quenching of the 5D state was found to be caused by collisions with caesium ground-state atoms. These results agree well with the data obtained by Sasso *et al* (1992), who performed experiments in both pulsed and cw regimes, and reported the values $\sigma_{43} = (55 \pm 25) \times 10^{-16}\ \mathrm{cm}^2$ and $\sigma_{\mathrm{D}} = (30 \pm 3) \times 10^{-16}\ \mathrm{cm}^2$ at $T = 480$–637 K (pulsed experiment), and $\sigma_{43} = (33 \pm 9) \times 10^{-16}\ \mathrm{cm}^2$ and $\sigma_{\mathrm{D}} = (26 \pm 12) \times 10^{-16}\ \mathrm{cm}^2$ at $T = 601$ K (cw experiment). In the evaluation of the results we used our own σ_{43} and σ_{D}, which almost coincide with the mean of the pulsed and cw values of Sasso *et al* (1992).

In the experiment we used both 6S $\rightarrow$ $5D_{5/2}$ and 6S $\rightarrow$ $5D_{3/2}$ excitation pathways. According to the model depicted in figure 3, the system of the steady-state rate equations for

the population densities N_1, N_2, N_3, and N_4 can be written in the following matrix form:

$$\begin{pmatrix} -(Z_1+R_{12}) & R_{21} & A_{31}+Q_{31} & Q_{41} \\ R_{12} & -(Z_2+R_{21}) & A_{32}+Q_{32} & A_{42}+Q_{42} \\ 0 & 0 & -(A_{3P}+Q_3+R_{34}) & R_{43} \\ 0 & 0 & R_{34} & -(A_{42}+Q_4+R_{43}) \end{pmatrix} \times \begin{pmatrix} N_1 \\ N_2 \\ N_3 \\ N_4 \end{pmatrix} = \begin{pmatrix} 0 \\ 0 \\ -P_3 \\ -P_4 \end{pmatrix}. \tag{17}$$

Here, $Z_1 = A_{10}^{eff} + Q_1$, $Z_2 = A_{20}^{eff} + Q_2$, $A_{3P} = A_{31} + A_{32}$, $Q_3 = Q_{31} + Q_{32}$, $Q_4 = Q_{41} + Q_{42}$, while P_3 and P_4 denote the pump rates. For $0 \rightarrow 3$ pumping rates P_3 and P_4 are $\rho B_{03} N_0$ and 0, respectively, while in the case of $0 \rightarrow 4$ pumping $P_3 = 0$ and $P_4 = \rho B_{04} N_0$.

The rates of interest were determined using the above system of steady-state rate equations and the data for population ratios N_i/N_j ($i = 1, 2, 3$, $j = 1, 2$). Using equations (14) and (16) for the evaluation, we obtained the relevant population ratios from measurements of relative intensities of the corresponding fluorescence lines.

According to data published by Sasso *et al* (1992) and our own (Vadla *et al* 1999), at caesium number densities of $\sim 5 \times 10^{14}$ cm^{-3} (typical for the 6P fine-structure mixing measurements), the quenching rates $Q_3 \approx Q_4$ are of the order of magnitude 5×10^4 s^{-1}, thus being negligible in comparison with the radiative rates $A_{31} = 9.0 \times 10^5$ s^{-1} and $A_{42} = 7.2 \times 10^5$ s^{-1}. Therefore, for this caesium density range these quenching rates can be omitted wherever they appear added to the spontaneous rates A_{31} or A_{42}. Within this approximation, the only remaining Q in the rate equation system (19) are Q_{32} and Q_{41}. The rate Q_{32} is most probably comparable with $A_{32} = 1 \times 10^5$ s^{-1}, while Q_{41} represents the exclusive population mechanism for the $4 \rightarrow 1$ transition. The values for Q_{32} and Q_{41} are unknown, and we were not able to determine their values from our experimental data. However, introducing the approximation $Q_3 \approx Q_4 = Q_D$ in the same *ad hoc* manner as in Sasso *et al* (1992), and assuming the equipartition in the branching of the quenching rates, we estimate both rates Q_{32} and Q_{41} to be equal to $Q_D/2$. Nevertheless, as will be shown eventually, this approximation has a minor influence on the final results. In this limit, using the principle of detailed balancing ($R_{21} = 1.93 R_{12}$ and $R_{34} = 1.18 R_{43}$ at $T_0 = 585$ K), from system (17) we obtain the following expressions for the ratio $m = Z_1/Z_2$ and the rates R_{12} and Z_2:

$$m = \frac{Z_1}{Z_2} = \frac{\xi h \frac{A_{31}}{A_{3P}} + t}{\eta + hp}, \tag{18}$$

$$R_{12} = \frac{m\eta - t}{(1+t)(1.93-\eta)} Z_2, \tag{19}$$

$$Z_2 = \chi \frac{A_{42} A_{3P}}{R_{43}} \frac{1+t}{1+m\eta}, \tag{20}$$

where

$$h = \frac{(1+t)(1.93-\eta)}{(1-1.93\xi)}, \tag{21}$$

$$t = \frac{A_{31} R_{43} + A_{3P} Q_D/2}{A_{3P} A_{42}}, \tag{22}$$

$$p = \frac{A_{32} + Q_D/2 + 1.18 R_{43}}{A_{3P}}. \tag{23}$$

The factors t and p can be calculated using the data listed above. The symbols η, ξ and

χ denote the population ratios $(N_1/N_2)_4$, $(N_2/N_1)_3$ and $(N_3/N_2)_4$, respectively, while the parenthesis index labels $0 \rightarrow 3$ or $0 \rightarrow 4$ pumping.

In this part of the experiment we measured the population density ratios η, ξ, and χ dependence on caesium ground-state number density. The η and ξ ratios suffice to determine the rate ratio m. The complete set of data for η, ξ, χ and m (each obtained as a function of N_0) enables the determination of the rates R_{12} and $Z_2 = A_{20}^{eff} + Q_2$. From the obtained ground-state density dependence of the rate R_{12} we determined the corresponding cross sections σ_{12} and $\sigma_{21} = 1.93\sigma_{12}$ (by the principle of detailed balance). The results for Z_2, in fact, yielded the values for the effective spontaneous rates, as will be shown in the following section.

3.2. Measurements and results

Figures 4(*a*) and (*b*) show the data for the relative populations of the $6P_J$ to $6P_{J'}$ and $5D_{3/2}$ to $6P_{3/2}$ states, respectively, obtained in series of measurements performed for caesium number densities in the range between 3×10^{14} and 3×10^{15} cm^{-3} at constant cell temperature $T_0 = 585$ K. For $0 \rightarrow 4$ excitation we measured the ratios $\eta = (N_1/N_2)_4$ and $\chi = (N_3/N_2)_4$, while in the case of $0 \rightarrow 3$ excitation the ratio $\xi = (N_2/N_1)_3$ was measured. The data were extracted from the spectra measured by scanning the monochromator, while the pump laser frequency was locked at the centre of the pump transition (see figure 2). The population ratios for the resonance substates were determined by measurements of relative intensities in the wings of the Cs D1 and Cs D2 lines for detuning $\Delta\lambda$ in the range from 1 to 2 nm. Equation (14) was used for the evaluation. To determine the $(N_3/N_2)_4$ ratio according to equation (16), the peak intensity I_{689} of the sensitized quadrupole line and the intensity $I_{3/2}(\Delta\lambda)$ in the blue wing of the Cs D2 line were measured. The spatial distributions of the excited atoms (see figure 5) were found to be independent of the caesium density range and the ratio of the volume integrals in equation (16) was 1.1.

Figures 6(*a*) and (*b*) show the results for $m = Z_1/Z_2$, Z_2 and R_{12} obtained by use of the data given in figure 4 for the lowest caesium densities. In this range, the mixing rate R_{12} exhibits linear dependence on caesium density. The error bars on the points in figures 6(*a*) and (*b*) reflect the error bars of the measured ratios η, ξ, and χ. The inaccuracy of the radiative and collisional rates used in evaluation were not included here. The apparently complicated formulae (18)–(23) used for evaluation imply a large overall uncertainty of the final results. The main contribution to the overall uncertainty of the final results is due to the factor $A_{42}A_{3P}/R_{43}$ appearing in expressions for evaluation of Z_2 and R_{12}. This factor directly scales the obtained results. Since the values for the radiative rates are very accurate ($\pm 5\%$), the largest error source is the rate R_{43}. However, the inaccuracies of the other similar terms have no such direct influence on the overall uncertainty of our results. This is due to the fact that the factors t and p comprising these terms are small compared with unity at lower caesium densities. For instance, at $N_0 = 5 \times 10^{14}$ cm^{-3} the factors t and p amount to 0.19 and 0.25, respectively. For this reason, our estimation $Q_3 \approx Q_4 = Q_D$ does not introduce major errors to the final result either. For example, a variation of $\pm 100\%$ in Q_D produces only $\pm 15\%$ uncertainty in Z_2 and R_{12}. Nevertheless, the error bars of the calculated values for m, Z_2, and R_{12} increase significantly for higher densities. Additionally, for higher densities our approximate solutions to the system (17) are no longer valid. Therefore, the data above $N_0 \sim 10^{15}$ given in figure 4 cannot be used for the evaluation.

The least-squares fit to the straight line through the origin of the first five experimental points for R_{12} in figure 6(*b*) yields the cross section $\sigma_{12} = R_{12}/v_{Cs-Cs}N_0$ for the process (2):

$$\sigma_{12} = (14 \pm 5) \times 10^{-16} \text{ cm}^2. \tag{24}$$

The error stated includes (adding in quadrature) the standard error of the fit obtained by

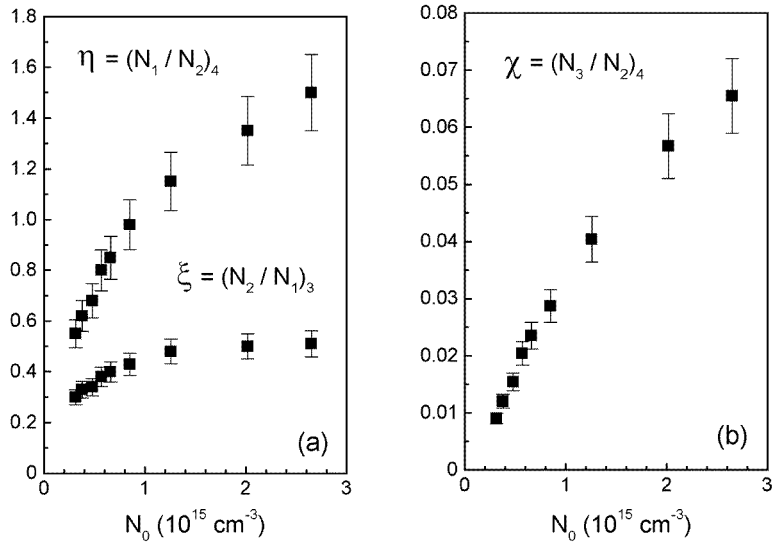

Figure 4. (*a*) The relative populations of the fine-structure levels of the Cs 6P state as a function of the caesium ground-state number density N_0. Ratios $\eta = N(6P_{1/2})/N(6P_{3/2})$ and $\xi = N(6P_{3/2})/N(6P_{1/2})$ were measured during the $6S_{1/2} \rightarrow 5D_{5/2}(0 \rightarrow 4)$ and $6S_{1/2} \rightarrow 5D_{3/2}(0 \rightarrow 3)$ excitations, respectively. (*b*) The population ratio $\chi = N(5D_{3/2})/N(6P_{3/2})$ in dependence on the caesium ground-state number density N_0 obtained for $0 \rightarrow 4$ excitation.

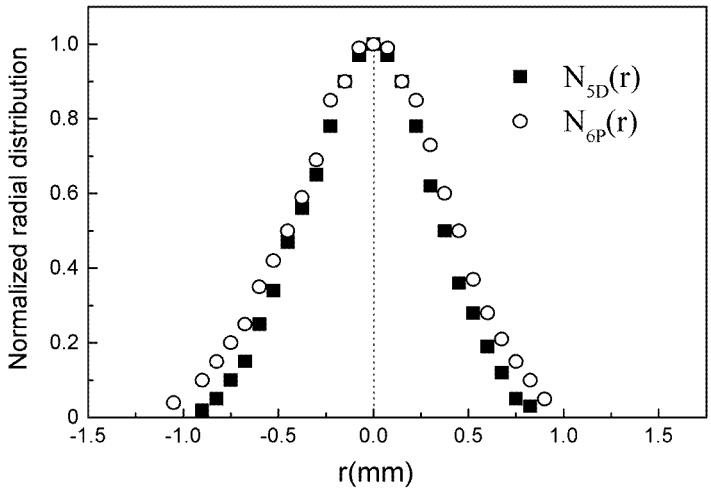

Figure 5. The normalized radial distributions $N(r)$ of caesium atoms excited to 5D and 6P states.

weighting the data by the experimental error bars (17%), the inaccuracy in the determination of the N_0 (5%) and the uncertainty of the rate R_{43} (33%) used in the evaluation. The value for the cross section σ_{21}, obtained from detailed balancing, amounts to 27×10^{-16} cm^2 (note that the evaluation procedure yields either of these two values; the other one follows from the principle of detailed balance). In table 1, the obtained values for σ_{12} and σ_{21} are compared with the results of previous investigations.

In order to estimate the radiative fraction of the depopulation rates $Z_i = A_{i0}^{eff} + Q_i$ we

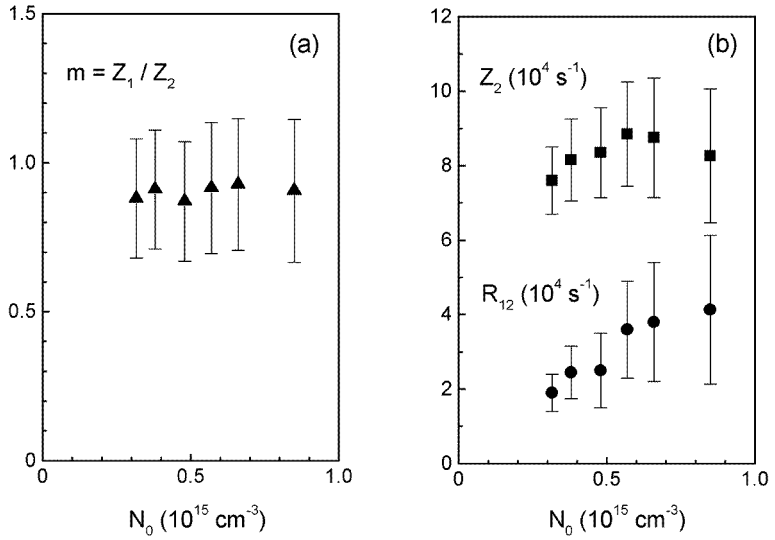

Figure 6. (*a*) The ratio m of the depopulation rates $Z_1 = A_{10}^{eff} + Q_1$ and $Z_2 = A_{20}^{eff} + Q_2$ of the fine-structure components of the Cs resonance level as a function of the ground-state number density N_0. (*b*) Depopulation rate Z_2 and mixing rate R_{12} plotted against the ground-state number density N_0. See section 3.1 for details.

Table 1. Cross sections for the fine-structure mixing of the Cs $6P_J$ states induced by collisions with ground-state caesium atoms.

Reaction	T (K)	σ (10^{-16} cm^2)	References
$Cs(6P_{1/2}) + Cs(6S_{1/2})$	473	6 ± 2	Bunke and Seiwert (1962)
$\rightarrow Cs(6P_{3/2}) + Cs(6S_{1/2})$	323	6.4 ± 0.6	Czajkowski and Krause (1965)
	585	14 ± 5	This work, experiment
	585	11	This work, theory
$Cs(6P_{3/2}) + Cs(6S_{1/2})$	473	13 ± 4	Bunke and Seiwert (1962)
$\rightarrow Cs(6P_{1/2}) + Cs(6S_{1/2})$	323	31 ± 3	Czajkowski and Krause (1965)
	585	27 ± 10	This work, from the experimental value and principle of detailed balance
	585	22	This work, from the calculated value and principle of detailed balance

calculated the effective radiative rates using Holstein's theory (Holstein 1947, 1951). In this experiment the distance between the centre of the excitation zone and the cell window was $r_0 \approx 0.5$ cm. For actual caesium densities, the kernel of the resonance line was thoroughly absorbed and only the resonance photons in the impact region of the self-broadened resonance line wings have a fair chance to escape out from the cell without being absorbed. For the case of cylindrical geometry and the impact region, the escape factor (the effective-to-natural radiative rate ratio) derived by Holstein (1947, 1951) is given by

$$G = \frac{A_{i0}^{eff}}{A_{i0}} = \frac{1.115}{\sqrt{\pi \kappa_p r_0}}, \tag{25}$$

where the Lorentzian peak absorption coefficient κ_p is given by

$$\kappa_p = \frac{\lambda_{i0}^2}{4\pi^2}\frac{g_i}{g_0}\frac{A_{i0}}{\Gamma_\nu}N_0. \tag{26}$$

According to Sobel'man *et al* (1981), the Lorentzian FWHM in our case is given by $\Gamma_\nu(\mathrm{s}^{-1}) = 2\pi^2 C_3(\mathrm{s}^{-1}\ \mathrm{cm}^3)N_0$. Using the values for the resonance interaction C_3 constants given by Horvatic *et al* (1993) and Movre and Pichler (1980), and the natural radiative rates $A_{10} = 2.84 \times 10^7\ \mathrm{s}^{-1}$ and $A_{20} = 3.24 \times 10^7\ \mathrm{s}^{-1}$ derived from Hansen (1984), we obtained $A_{10}^{eff} \approx A_{20}^{eff} = 8.4 \times 10^4\ \mathrm{s}^{-1}$. Since our experimental Z_2 value reads $Z_2 = (8.3 \pm 1.5) \times 10^4\ \mathrm{s}^{-1}$, this theoretical estimate indicates that for the actual caesium density range the measured depopulation rates are dominated by the effective radiative rates, while the quenching rates Q_1 and Q_2 are negligible within the experimental error bar. As predicted by Holstein's theory (Holstein 1947, 1951), the effective radiative rates at present conditions are independent of the ground-state atom density and their ratio is nearly equal to unity. From the experiment we obtained $m = Z_1/Z_2 = 0.9 \pm 0.2$, which is in fair agreement with the theoretical prediction.

4. Quenching of the $6P_J$ states

4.1. Rate equations and methods

As shown in the previous section, the collisional depopulation rates Q_1 and Q_2 of the $6P_{1/2}$ and $6P_{3/2}$ states, respectively, were not measurable in the low caesium density range. To get information about these rates, we performed a separate set of measurements at higher densities ranging between 1×10^{16} and $5 \times 10^{16}\ \mathrm{cm}^{-3}$. The cell temperature was kept at $T_0 = 635$ K, which is about 30 K higher than the highest metal bath temperature in this part of the experiment. We found that for caesium densities above $1 \times 10^{16}\ \mathrm{cm}^{-3}$ complete mixing of the $6P_J$ states occurred. For this reason, it is convenient to reduce the system (17) (by adding together the first two equations) to a simpler three-state form with relevant populations $N_\mathrm{P} = N_1 + N_2$, N_3, and N_4. Then, for $0 \rightarrow 4$ pumping the corresponding rate equation system in matrix form is

$$\begin{pmatrix} -Z_\mathrm{P} & A_{3\mathrm{P}} + Q_\mathrm{D} & A_{42} + Q_\mathrm{D} \\ 0 & -(A_{3\mathrm{P}} + Q_\mathrm{D} + R_{34}) & R_{43} \\ 0 & R_{34} & -(A_{42} + Q_\mathrm{D} + R_{43}) \end{pmatrix} \times \begin{pmatrix} N_\mathrm{P} \\ N_3 \\ N_4 \end{pmatrix} = \begin{pmatrix} 0 \\ 0 \\ -\rho B_{04} N_0 \end{pmatrix}. \tag{27}$$

Here, $Z_\mathrm{P} = [Z_1 + (N_1/N_2)Z_2]/[1 + (N_1/N_2)]$ is effective depopulation rate of the 6P state, and we use again the approximation $Q_3 \approx Q_4 \equiv Q_\mathrm{D}$.

The equilibrium ratio N_1/N_2 at $T = 635$ K amounts to 1.72 and the total $6P_J$ population density N_P amounts to $2.72N_2$. The system (27) yields the depopulation rate of the 6P state:

$$Z_\mathrm{P} = \frac{1}{2.72}\left(\frac{N_3}{N_2}\right)_4 \left[A_{3\mathrm{P}} + Q_\mathrm{D} + (A_{42} + Q_\mathrm{D})\frac{A_{3\mathrm{P}} + Q_\mathrm{D} + 1.17R_{43}}{R_{43}}\right], \tag{28}$$

where, according to the principle of detailed balance, we used $R_{34} = 1.17R_{43}$ at $T = 635$ K.

The ratio $\chi = (N_3/N_2)_4$ was measured in dependence on the caesium ground-state number density. Using these data we calculated the Z_P in dependence on N_0. Generally, the rate Z_P is a sum of the effective radiative depopulation rate and the quenching rates due to collisions with caesium atoms and molecules:

$$Z_\mathrm{P} = A_\mathrm{P}^{eff} + \sigma_\mathrm{P}^a v_{a-a} N_0 + \sigma_\mathrm{P}^m v_{a-m} N(\mathrm{Cs}_2). \tag{29}$$

Here, σ_{P}^{a} and σ_{P}^{m} are the cross sections for the atomic and molecular quenching, respectively. Since the density of the caesium molecules is related to the N_0 by a temperature-dependent equilibrium rate $K_{eq}(T)$ through

$$N(\mathrm{Cs}_2) = \frac{N_0^2}{K_{eq}(T)}, \tag{30}$$

the depopulation rate Z_{P} can be, in terms of N_0, represented by a second-order polynomial:

$$Z_{\mathrm{P}} = b_0 + b_1 N_0 + b_2 N_0^2. \tag{31}$$

By fitting the experimental data for Z_{P} to the second-order polynomial, the quenching cross sections can be obtained from derived coefficients b_i as $\sigma_{\mathrm{P}}^{a} = b_1/v_{a-a}$ and $\sigma_{\mathrm{P}}^{m} = b_2 K_{eq}(T)/v_{a-m}$. For the evaluation of the molecular cross section we used $K_{eq}(T)$ calculated according to the expression

$$K_{eq}(T) = 1.37 \times 10^{22} \times T^{1/2} \times \exp(-5.22 \times 10^3/T) \times [1 - \exp(-60.46/T], \tag{32}$$

obtained by use of caesium molecular ground-state constants given by Weickenmeier *et al* (1985).

4.2. Measurements and results

Figure 7(*a*) shows the population ratio $\chi = (N_3/N_2)_4$ measured in dependence on caesium ground-state number density. To avoid excessive population density in the 6P states and trapping of the 5D $\rightarrow$ 6P transition, the pump power was reduced down to 5 mW. The ratio χ was determined according to equation (16), by measuring the peak intensity of the sensitized 689 nm quadrupole line and the intensity in the blue wing of the Cs D2 line for detuning $\Delta\lambda$ in the range from 3 to 7 nm. The transparency of the cell windows reduces equally at both wavelengths of interest (852 and 689 nm), leaving the intensity ratio unaffected by its change. Using these data and equation (28) we calculated the Z_{P} dependence on caesium ground-state atom density. The rates R_{43} and Q_{D} were calculated using our σ_{43} and σ_{D} values given in section 3.1. The results for the depopulation rate Z_{P} of the 6P states are plotted in figure 7(*b*) against caesium atom number density N_0. Figure 7(*c*) displays the Z_{P} data versus density of caesium molecules N_{Cs_2}. The Z_{P} versus N_{Cs_2} plot is quite instructive, since it shows that Z_{P} is almost a linear function of N_{Cs_2} and we can tell at a glance that in the investigated Cs density range, except for the narrow interval at the very beginning, the Z_{P} is dominated by the molecular quenching.

By fitting the data presented in figure 7(*b*) to the second-order polynomial (equation (31)) we obtained the following values for the coefficients: $b_0 = (1.6 \pm 0.7) \times 10^5$ s^{-1}, $b_1 = (7.0 \pm 6.3) \times 10^{-12}$ s^{-1} cm^3, $b_2 = (5.6 \pm 1.2) \times 10^{-28}$ s^{-1} cm^6. The fitting was done by the least square method using the plotted error bars as weights for the data. The plotted error bars include the uncertainties in χ as well as the errors in the cross sections used for evaluation of Z_{P}.

The coefficient b_0 gives the effective radiative rate A_{P}^{eff} which is two times greater than the value obtained in the course of 6P fine-structure mixing measurements (section 3.2). However, taking into account the overlapping error bars of these data, they may be regarded as consistent. With the relative velocity $v_{a-a} = 4.5 \times 10^4$ cm s^{-1} we obtain from b_1 the following value for the atomic quenching cross section:

$$\sigma_P^a = (1.6 \pm 1.4) \times 10^{-16}\ \mathrm{cm}^2. \tag{33}$$

At the experimental temperature $K_{eq}(635) = 8.44 \times 10^{18}$ cm^3, while the relative velocity between caesium atoms and molecules amounts to $v_{a-m} = 3.9 \times 10^4$ cm s^{-1}. Using these

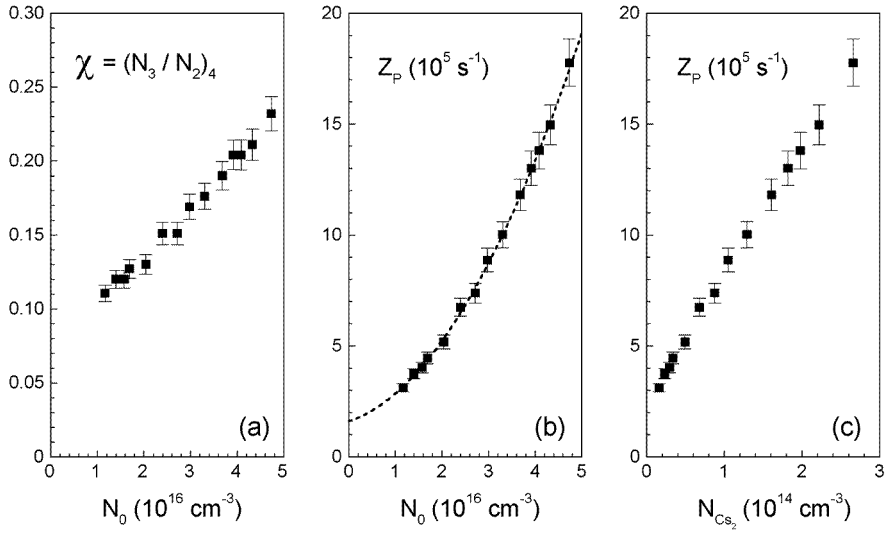

Figure 7. (*a*) The population ratio $\chi = N(5D_{3/2})/N(6P_{3/2})$ in dependence on the caesium ground-state number density N_0 obtained for $0 \rightarrow 4$ excitation, measured in the range of higher N_0 densities. (*b*) Total depopulation rate Z_P of the 6P state plotted against the ground-state number density N_0. The dashed curve represents equation (31). (*c*) Total depopulation rate Z_P of the 6P state plotted against the number density of caesium molecules N_{Cs_2}.

Table 2. The cross sections for quenching of the Cs 6P state induced by collisions with caesium ground-state atoms and molecules.

Reaction	T (K)	σ (10^{-16} cm^2)	References
Cs(6P) + Cs(6S) $\rightarrow$ Cs(6S) + Cs(6S)	480–637	6.6 ± 3	Sasso *et al* (1992)
	480–637	2.1	Huennekens and Sasso (1998)
	635	1.6 ± 1.4	This work, experiment
	635	<16	This work, theory
Cs(6P) + Cs_2 $\rightarrow$ Cs(6S) + Cs_2^*	480–637	863 ± 260	Sasso *et al* (1992)
	480–637	546	Huennekens and Sasso (1998)
	635	1210 ± 260	This work, experiment

data, from the coefficient b_2, we obtain the following value for the molecular quenching cross section:

$$\sigma_P^m = (1210 \pm 260) \times 10^{-16}\ \text{cm}^2. \tag{34}$$

The values for σ_P^a and σ_P^m are listed in table 2 and compared with those measured by Sasso *et al* (1992).

As mentioned previously, the atomic quenching rate includes not only the collisional excitation transfer to the ground state described by (4) but also the collisional back transfer to the 5D states. To estimate the back-transfer component of the measured cross section σ_P^a we used the principle of detailed balancing. At the temperature at hand, the ratio σ_D'/σ_D is equal to 2×10^{-3} (σ_D' denotes the cross section for the 6P $\rightarrow$ 5D back transfer), and according to the values (Sasso *et al* 1992, Vadla *et al* 1999) for σ_D mentioned in section 3.1, the cross section σ_D' amounts to 0.06×10^{-16} cm^2. This means that the measured quenching cross section σ_P^a should be completely attributed to the process Cs(6P) + Cs(6S) $\rightarrow$ Cs(6S) + Cs(6S).

5. Discussion

5.1. Mixing of the $6P_J$ states

The first experimental investigation of the fine-structure mixing of the Cs 6P states due to collisions with ground-state Cs atoms was performed by Bunke and Seiwert (1962), who reported $\sigma_{1/2\to3/2} = (6 \pm 2) \times 10^{-16}$ cm^2 and $\sigma_{3/2\to1/2} = (13 \pm 4) \times 10^{-16}$ cm^2 at $T = 473$ K. This process was remeasured by Czajkowski and Krause (1965) who found $\sigma_{1/2\to3/2} = (6.4 \pm 0.6) \times 10^{-16}$ cm^2 and $\sigma_{3/2\to1/2} = (31 \pm 3) \times 10^{-16}$ cm^2 at $T = 323$ K. Bunke and Seiwert (1962) worked at Cs ground-state densities of $\sim 10^{15}$ cm^{-3} and corrected their results for radiation trapping by using a modified Holstein theory (Holstein 1947). On the other hand, the experiment of Czajkowski and Krause (1965) was performed in optically thin conditions and required no corrections for trapping of the resonance radiation. Both experiments were done by means of classical spectroscopy, and no attempt to measure these cross sections by laser spectroscopy methods has been done since. The ratio of the cross sections measured by Czajkowski and Krause (1965) agrees very well with the value calculated by the principle of detailed balancing, while that of Bunke and Seiwert (1962) is about 20% higher than predicted by detailed balancing. These two results suggest that the cross section for the endothermic process $6P_{1/2} \to 6P_{3/2}$ decreases slightly, while the cross section for the exothermic $6P_{3/2} \to 6P_{1/2}$ process rapidly decreases with temperature (by more than a factor of two in the considered temperature range). This is not in accordance with the expectation that cross sections for endothermic reactions increase, while cross sections for exothermic processes mildly decrease with increased temperature (see the discussion in Vadla (1998)).

There are three basic mechanisms which can contribute to the fine-structure-changing collision cross section for the first excited P state in the homonuclear alkali dimers at room temperature. Only one, the spin–orbit mixing of the 0_u^+ components of the $A\,^1\Sigma_u^+$ and $b\,^3\Pi_u^+$ states at their crossing near the minimum of the $A\,^1\Sigma_u^+$ potential, is dominant in the Cs case (Julienne and Vigué 1991). Using the nonrelativistic potentials of Krauss and Stevens (1990) and the spin–orbit matrix element estimated by O'Callahan *et al* (1985), Julienne and Vigué (1991) have calculated the cell average cross section for Cs fine-structure-changing collisions at 300 K, obtaining the value $\sigma_{3/2\to1/2} = 33.6\times10^{-16}$ cm^2. They also showed that the temperature dependence of the fine-structure rate coefficient is that of the Langevin capture rate, i.e. $T^{-1/6}$. It follows that the temperature dependence of the corresponding thermal cross section is $T^{-2/3}$. The theoretical value for $T = 300$ K scaled to $T = 585$ K yields $\sigma_{3/2\to1/2} = 21.5\times10^{-16}$ cm^2 and by using the principle of detailed balancing, $\sigma_{1/2\to3/2} = 11.0 \times 10^{-16}$ cm^2, which is in good agreement with our measured value of $(14 \pm 5) \times 10^{-16}$ cm^2.

When our present results $\sigma_{1/2\to3/2} = (14 \pm 5) \times 10^{-16}$ cm^2 and $\sigma_{3/2\to1/2} = (27 \pm 10) \times 10^{-16}$ cm^2 obtained at $T = 585$ K are incorporated into the scheme of existing data it is possible to resolve the inconsistency between previously (Bunke and Seiwert 1962, Czajkowski and Krause 1965) reported values. The Cs 6P fine-structure mixing cross sections are depicted in figure 8 together with previous experimental results (Bunke and Seiwert 1962, Czajkowski and Krause 1965) and the theoretical predictions (Julienne and Vigué 1991) for their temperature dependence. It can be seen that only the data of Czajkowski and Krause (1965), together with our present ones, reproduce the theoretical predictions. It is also clear that the results of Bunke and Seiwert (1962) are systematically about a factor of two too low to fit reasonably into the body of existing values. This is not surprising, bearing in mind the assumptions about the geometry of their system that were necessary in order to account for radiation trapping. The present experiment also proceeded under conditions of radiation trapping, the important distinction being that the method we applied enabled direct experimental determination of

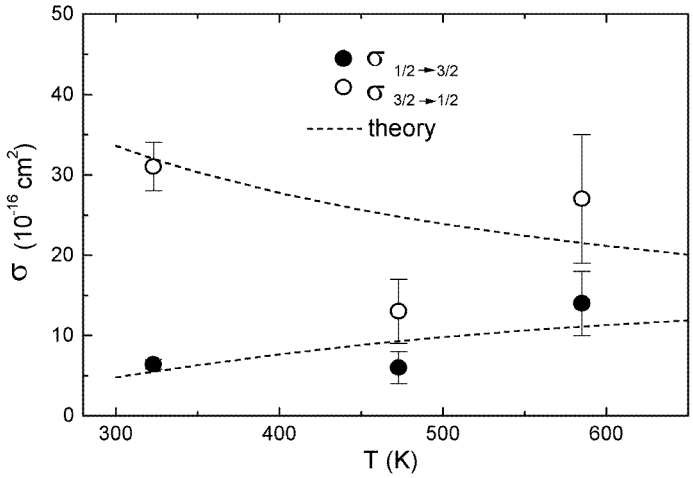

Figure 8. Temperature dependence of the Cs 6P fine-structure mixing cross sections: $T = 323$ K, Czajkowski and Krause (1965); $T = 473$ K, Bunke and Seiwert (1962); $T = 585$ K, present experiment; dashed curves, theory (Julienne and Vigué 1991).

the effective radiative rates for 6P levels, simultaneously with measurements of the mixing rates. This method is advantageous since it circumvents the necessity of applying any theory of radiation trapping in advance.

5.2. Quenching of the $6P_J$ states

To our knowledge there is a single result in the literature, by Sasso *et al* (1992), for the quenching cross sections of the Cs 6P state. They reported the cross sections $\sigma_{at} = (6.6 \pm 3) \times 10^{-16}$ cm^2 and $\sigma_{mol} = (863 \pm 260) \times 10^{-16}$ cm^2, for quenching by caesium ground-state atoms and molecules, respectively, in the temperature range 480–637 K. Our result ($T = 635$ K) for the atomic quenching cross section $\sigma_{at} = (1.6 \pm 1.4) \times 10^{-16}$ cm^2 is about four times smaller, while the molecular quenching cross section $\sigma_{mol} = (1210 \pm 260) \times 10^{-16}$ cm^2 is about 40% greater than that reported by Sasso *et al* (1992). We attempted to find a cause of such great disagreement between the results for atomic quenching by analysing the conditions in which the two experiments were performed. Sasso *et al* (1992) performed the measurements in the heat pipe, while we used a glass cell where the possible influence of impurities is much less likely. However, we do not consider either this difference or the different techniques used (cw and pulsed), to be the essential cause of the disagreement. In our opinion it is more likely that basic experimental conditions which were different in the two experiments are responsible for the disagreement. Our measurements were made under conditions of complete mixing of the 6P states, while the measurements of Sasso *et al* (1992) also include the range of low caesium densities far removed from the mixing saturation, where the measured outgoing rate of the particular observed $6P_J$ state is predominantly governed by the 6P intermultiplet mixing mechanism (see equation (14) in Sasso *et al* (1992)). Furthermore, the caesium vapour temperature in their experiment changed simultaneously with the caesium number density, since the experiment was performed in the heat pipe. As a consequence, the data obtained had to be fitted to a second-order polynomial (equivalent to our equation (31)) in which the coefficient of the quadratic term was temperature dependent (with one order of magnitude change in the considered temperature range). In contrast, by using a sealed glass cell we

were able to investigate these processes at a constant caesium vapour temperature. Therefore, our Z_P versus N_0 data follow a true parabola, thus making our fitting (figure 7(*b*)) procedure simpler and *a priori* more reliable.

In attempting to compare our results with the results of Sasso *et al* (1992), we noticed that the declared cross sections were incompatible with the experimental data points given in that work. Recently (Huennekens and Sasso 1998), we have learned that the quenching cross sections $\sigma_P(Cs)$ and $\sigma_P(Cs_2)$ reported by Sasso *et al* (1992) are in error, and that the correct values should read 2.1×10^{-16} cm^2 and 546×10^{-16} cm^2. We do not know whether the corresponding error bars represent the same percentage as the original values or not. Both data sets are listed in table 2. Taking the recent (Huennekens and Sasso 1998) values into consideration, we can see that there is now a good agreement between the cross sections for atomic quenching, but that the disagreement between the cross section values for molecular quenching is even worse than before. We cannot think of any reason, other than those already discussed, that would account for this discrepancy.

According to Nikitin and Shushin (1977), in the alkali homonuclear systems the quenching of the first excited P state is due to rotational and spin–orbit coupling between the a $^3\Sigma_u^+$ and the b $^3\Pi_u$ potential curves which cross each other at short internuclear distances (see figure 9). In the simple two-channel model the transition probability is given by the Landau–Zener formula:

$$P_{LZ} = 2e^{-A}(1 - e^{-A}) \tag{35}$$

where

$$A = 2\pi V_x^2/(\hbar v_x D_x) \tag{36}$$

and V_x, v_x and D_x are respectively the coupling matrix element, velocity and slope difference of the potential curves at the crossing point R_x of the two curves. The selection rules for the two couplings are different and the total quenching cross section is given as a sum of two contributions. In the case of the rotational (Coriolis) coupling, the Landau–Zener treatment would be applicable, provided that the coupling is not too strong (Nikitin and Umanskii 1984). If so, then $A \ll 1$, and $P_{LZ} = 2A$. The Coriolis coupling matrix element is of the form $V = -(bv_\infty/R^2)\langle {}^3\Sigma_u^+|\hat{L}_\perp|{}^3\Pi_u\rangle$, where b is the impact parameter, v_∞ is the asymptotic velocity in the initial channel and $\hat{L}_\perp$ is that component of the electronic angular momentum operator which is perpendicular to the collision plane. Assuming that the molecular wavefunctions of the $^3\Sigma$ and the $^3\Pi$ states are dominated by 6s and 6p atomic orbitals, both (rotational and spin–orbit) coupling matrix elements take the form of the product of the respective asymptotic value and a common factor $f(0 < f < 1)$ which comprises the amplitudes of the pσ and pπ atomic orbitals in the molecular wavefunctions of the Σ and Π states (Nikitin and Shushin 1977).

Krauss and Stevens (1990) have calculated adiabatic potential energy curves of Cs_2 in the range of internuclear distances R from 7 to 30 a_0. In order to estimate the crossing of the relevant potential curves in the range of shorter internuclear distances where quantum chemical methods usually lose accuracy we have extrapolated calculated potential curves by simple exponentials. The extrapolation yields the crossing at $R_x = 5.94\ a_0$ and energy $U_x = -0.011\,545 E_h$ relative to the S+P asymptote (see figure 9). Using these values we have calculated the transition probability according to equation (35). The quenching cross section, as a function of the factor f, is then obtained by integrating transition probability over impact parameter and averaging over Maxwellian energy distribution. In variance with the K_2 case (Nikitin and Shushin 1997), quenching of the Cs 6P states is almost exclusively given by the spin–orbit coupling. The (atomic) quenching cross section, as a function of f, exhibits a maximum of 16×10^{-16} cm^2 for $f = 0.6$. This f value is rather unrealistic since

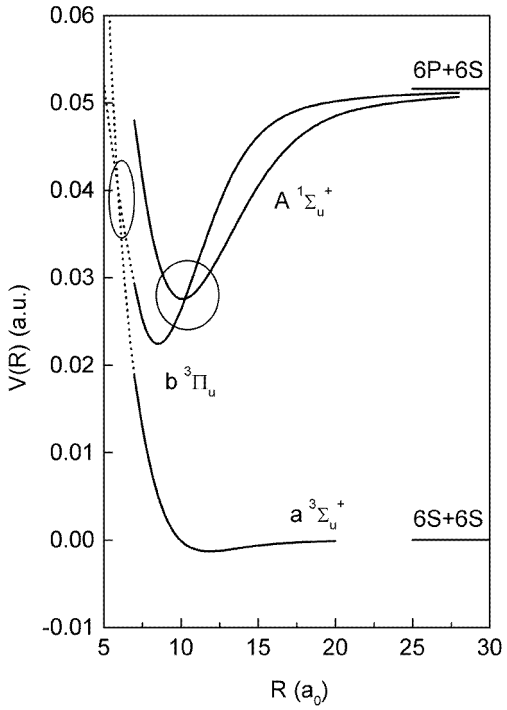

Figure 9. Some of the nonrelativistic potential curves for Cs_2 calculated by Krauss and Stevens (1990). The dotted curves represent our extrapolation of a $^3\Sigma_u^+$ and b $^3\Pi_u$ potentials. The circled areas indicate the crossings considered in section 5.1.

it would imply that the wavefunction of the a $^3\Sigma_u^+$ state is dominated by the pπ atomic orbital, which is not very likely. Therefore, when judging the agreement between the theory and the experimental values, the theoretical upper bound of 16×10^{-16} cm^2 should not be given much significance, prior to knowing the f value more reliably. The experimental findings for this quenching cross section suggest that f should be about 0.1.

The dynamics of the collision is a complex problem not only because a large number of electronic states may be involved but also due to the sensitivity to details of the potential curves. In addition, the knowledge of various coupling matrix elements is required. To our best knowledge, no radial or rotational coupling matrix elements are available in the literature. Better insight into the collision dynamics of these processes certainly requires more complete theoretical treatment, which, however, is beyond the scope of this paper.

6. Conclusion

EET processes involving caesium atoms excited to the 6P state and colliding with the caesium ground-state atoms or molecules have been investigated. We have measured the cross section

$$\sigma_{1/2\to 3/2} = (14 \pm 5) \times 10^{-16}\ \text{cm}^2$$

for the fine-structure mixing of the Cs 6P$_J$ states ($T = 585$ K) induced by collisions with ground-state caesium atoms. Our theoretical estimate for this process, based on the value calculated by Julienne and Vigué (1991), yields $\sigma_{1/2\to 3/2} = 11 \times 10^{-16}$ cm^2. The experimental value is consistent with the results previously reported by Czajkowski and Krause (1965).

The cross sections $\sigma_P^a = (1.6 \pm 1.4) \times 10^{-16}$ cm^2 and $\sigma_P^m = (1210 \pm 260) \times 10^{-16}$ cm^2 for the quenching of the Cs 6P state by collisions with caesium ground-state atoms and molecules, respectively, have been determined at the temperature $T = 635$ K. The value for the atomic quenching cross section communicated to us by Huennekens and Sasso (1998) is in good agreement with the result reported here, while their molecular quenching cross section is about two times smaller.

Finally, we would like to point out the need for further theoretical investigation of the Cs_2 collisional complex, which should include not only potential curves but also the various coupling elements relevant for cross section calculations.

Acknowledgments

The authors wish to thank J Huennekens for valuable comments during the preparation of the manuscript. This research was supported by the Ministry of Science and Technology of the Republic of Croatia.

References

Bunke H and Seiwert R 1962 *Optik und Spektroskopie aller Wellenlängen* (Berlin: Akademie)
Czajkowski M and Krause L 1965 *Can. J. Phys.* **43** 1259
Hansen W 1984 *J. Phys. B: At. Mol. Phys.* **17** 4833
Holstein T 1947 *Phys. Rev.* **72** 1212
——1951 *Phys. Rev.* **83** 1159
Horvatic V, Movre M, Beuc R and Vadla C 1993 *J. Phys. B: At. Mol. Opt. Phys.* **26** 3679
Huennekens J and Sasso A 1998 Private communication
Jabbour Z J, Namiotka R K, Huennekens J, Allegrini M, Milosevic S and de Tomasi F 1996 *Phys. Rev.* A **54** 1372
Julienne P S and Vigué J 1991 *Phys. Rev.* A **44** 4464
Krause L 1975 *The Excited State in Chemical Physics* ed J W McGowan (New York: Wiley) pp 267–316
Krauss K and Stevens W J 1990 *J. Chem. Phys.* **93** 4236
Link J K 1966 *J. Opt. Soc. Am.* **56** 1195
Marinescu M and Dalgarno A 1995 *Phys. Rev.* A **52** 311
Mitchell A C G and Zemansky M W 1971 *Resonance Radiation and Excited Atoms* (Cambridge: Cambridge University Press)
Movre M and Pichler G 1977 *J. Phys. B: At. Mol. Phys.* **10** 2631
——1980 *J. Phys. B: At. Mol. Phys.* **13** 697
Niemax K 1977 *J. Quant. Spectrosc. Radiat. Transfer* **17** 125
Nikitin E E and Shushin A I 1977 *Opt. Spektrosk. (USSR)* **43** 235
Nikitin E E and Umanskii S Ya 1984 *Theory of Slow Atomic Collisions* (Berlin: Springer)
O'Callahan M J, Gallagher A and Holstein T 1985 *Phys. Rev.* A **32** 2754
Rafac R J, Tanner C E, Livingston A E, Kukla K W, Berry H G and Kurtz C A 1994 *Phys. Rev.* A **50** R1976
Sasso A, Demtröder W, Colbert T, Wang C, Ehrlacher E and Huennekens J 1992 *Phys. Rev.* A **45** 1670
Sobel'man I I, Vainshtein L A and Yukov E A 1981 *Excitation of Atoms and Broadening of Spectral Lines* (Berlin: Springer)
Tanner C E, Livingston A E, Rafac R J, Serpa F G, Kukla K W, Berry H G, Young L and Kurtz C A 1992 *Phys. Rev. Lett.* **69** 2765
Vadla C 1998 *Eur. Phys. J.* D **1** 259
Vadla C, Movre M and Horvatic V 1999 *Fizika* A submitted
Vadla C, Niemax K and Brust J 1996 *Z. Phys.* D **37** 241
Weickenmeier H, Diemer U, Wahl M, Raab M, Demtröder W and Müller W 1985 *J. Chem. Phys.* **82** 535
Young L, Hill W T III, Sibener S J, Price S D, Tanner C E, Wieman C E and Leone S R 1994 *Phys. Rev.* A **50** 2174